Supplementary information for:

The role of traffic emissions in particulate organics and nitrate at a downwind site in the periphery of Guangzhou, China

Yi Ming Qin[1], Hao Bo Tan[2], Yong Jie Li[3,*], Misha I. Schurman[4], Fei Li[2], Francesco Canonaco[5], André S. H. Prévôt[5], Chak K. Chan[1,4,6,*]

[1]Department of Chemical and Biomolecular Engineering, Hong Kong University of Science and Technology, Hong Kong, China

[2]Institute of Tropical and Marine Meteorology, China Meteorological Administration, Guangzhou, China

[3]Faculty of Science and Technology, University of Macau, Taipa, Macau, China

[4]Division of Environment, Hong Kong University of Science and Technology, Hong Kong, China

[5]Laboratory of Atmospheric Chemistry, Paul Scherrer Institute, 5232, Villigen PSI, Switzerland

[6]School of Energy and Environment, City University of Hong Kong, Hong Kong, China

[*]To Whom Correspondence Should be Addressed

Chak K. Chan: AC1-G5716, School of Energy and Environment, City University of Hong Kong,
Tat Chee Avenue, Kowloon, Hong Kong, China
Tel: (852) 3442-5593; Fax: (852) 3442-0688
Email: chak.k.chan@cityu.edu.hk

Yong Jie Li: E11-3017, Faculty of Science and Technology, University of Macau, E11, Avenida da
Universidade, Taipa, Macau, China
Tel: (853) 8822-4943; Fax: (853) 8822-2426
Email: yongjieli@umac.mo

1 **Text:**

2 **Text S1:** Diurnal Patterns of meteorological conditions and gas and particle species.

3   Diurnal patterns for temperature, RH, irradiance (IR), NO_x, O_3, all NR-PM_1 species, and BC in

4 November and December are depicted in Figure S11. IR, an indicator of photochemical activities,

5 showed a clear noon time peak in November. Ozone concentration is also closely linked to the

6 extent of photochemical oxidation in an air mass because O_3 production results from OH reactions

7 with VOCs and CO. In general, ozone concentration slowly increases after sunrises and reaches

8 its maximum in mid-afternoon. In November, both IR and O_3 were relatively high at noon time,

9 indicating the strong photochemical activities. Obvious diurnal cycles of temperature and RH were

10 observed. SO_2 had morning peaks while NO_x showed clear rush hour peaks. Sulfate showed a

11 slight concentration increase in median hourly data in the early morning in November, consistent

12 with the SO_2 morning peaks. The daytime decrease in nitrate and chloride in November may due

13 to the combinative effects of higher mixing layer height and gas-to particle partitioning under high

14 temperature and low RH conditions (Seinfeld and Pandis, 2006). Ammonium concentration

15 decreased in the early morning and increased in late afternoon, which was the combined result of

16 the variations of anions in the particle (SO_4, NO_3 and Chl). Organics had a significant increase

17 after 16:00, and stayed at a high level at night, which might be attributed to combined effects of

18 enhanced vehicular emissions and lower mixing layer height. Other vehicle-related pollutants such

19 as NO_x and BC also showed an increase in concentrations after 16:00. Also, a small organics peak

20 appeared in the afternoon, coincided with the peak of O_3, suggesting the possibility of

21 photochemical formation of SOA. The diurnal patterns of individual organic factors as

22 characterized by ME-2 which will be discussed in a later section. Similar diurnal variations for

23 most of the PM_1 species in November were also observed in the earlier field campaign conduced

24 in November in Shenzhen (He et al., 2011).

25   In December, although O_3 concentrations were significantly lower than those in November, the

26 daytime peak was still obvious. Both temperature and RH were lower in December than in

27 November while obvious diurnal cycles of temperature and RH were also observed. No obvious

28 diurnal variation for SO_2 were observed in December. NOx still showed clear rush hour peaks.

29 However, a discrepancy between mean and median data in diurnal patterns for NO_x was apparent

30 during night to early morning in December because of intense traffic emissions on 24-25

31   December, as also shown in the high NO_x concentrations in Figure 1. SO_4 slightly increased at

32   night, which might be attributed to the lower mixing layer height during nighttime. However,

33   nitrate concentration did not experience a significant decrease, while the daytime decrease in

34   chloride is still obvious. Other contributing factors of nitrate may somewhat offset the decrease

35   due to higher mixing layer height and evaporation from particles in daytime. Ammonium

36   concentration increased in late afternoon, which was the combined result of the variations of anions

37   in the particle. Organics had a significant increase after 16:00, stayed at a high level at night, and

38   tracked well with vehicle-related pollutants such as NO_x and BC.

39   Text S2: Organic nitrate and inorganic nitrate estimation

40   To exanimate the contribution of organic nitrate (ON) to nitrate measured by the HR-ToF-AMS,

41   we adopted two methods to estimate the ON concentration. The first method (Method 1) is based

42   on the ratio of NO^+/NO_2^+ (Farmer et al., 2010), which makes use of the difference in NO^+/NO_2^+

43   ratios for organic nitrates and ammonium nitrate in the AMS spectra. The fraction of the total

44   nitrate signal due to organic nitrates (x) can be derived from:

45    $$x = \frac{(R_{obs} - R_{NH4NO3})(1 + R_{ON})}{(R_{ON} - R_{NH4NO3})(1 + R_{obs})} \quad (1)$$

46   where R_{obs} is the NO^+/NO_2^+ ratio in the mass spectra, R_{NH4NO3} is the NO^+/NO_2^+ ratio of ammonium

47   nitrate in IE calibrations, while R_{ON} is the NO^+/NO_2^+ ratio of ON. Xu et al.(2015) used the

48   NO^+/NO_2^+ ratios of 5 and 10, which likely correspond to the upper and lower bounds of the ratios

49   from ON. This method using NO^+/NO_2^+ is adopted in this study for the estimation of contributions

50   for organic nitrates to the AMS-measured nitrate signals. The concentrations of organic nitrates

51   can be derived by multiplying the organic nitrate fraction (x) with the total nitrate measured by the

52   AMS. And inorganic nitrate can then be calculated by subtracting the organic nitrates from the

53   total nitrate concentrations. But still, we should be cautious when using this method, as the vast

54   array of possible ON parent compounds in ambient particles and the variation of the NO^+/NO_2^+

55   ratios between instruments may led to some bias in the calculation. We also use the organic

56   concentrations and elemental ratios (OM:OC and N:C) from the HR-ToF-AMS measurement to

57   estimate the lower bound of concentrations for organic nitrates   (Method 2) adopted from

58   Schurman et al.(2015).

59   ON_{min}=(Organics/OM:OC)*N: C*(14/12) (2)

60   where Organics is total organic concentration. ON may be underestimated using this method as

61   N:C includes only N from CHON and CHN fragments. The maximum inorganic nitrate can also

62   be estimated by deducting the ON_{min} from the total nitrate concentration using this method.

63   The time series of total nitrate form AMS and MAGRA, and inorganic nitrate and organic nitrate

64   calculated from Method 1 and Method 2 are shown in Fig. S12, while the campaign average mass

65   concentration and mass fraction derived from each method are shown in Fig. S13-S14. On average,

66   the maximum IN concentration estimated from Method 1 was 6.15 $\mu g/m^3$, accounted for 81.2% of

67   the total nitrate mass concentration from AMS measurement. And the minimum IN concentration

68   from Method 1 was 4.95 $\mu g/m^3$, contributed to 74.4% of the total nitrate mass. While using Method

69   2, the minimum nitrate was 6.48 $\mu g/m^3$, accounted for 89.8 % of the total nitrate. And the time

70   series of the calculated inorganic nitrate tracked well with the total AMS measured nitrate (Fig.

71   S12). Fig. 8 shows the scatter plot of estimated inorganic nitrate versa total AMS measured nitrate.

72   We found that the estimated inorganic nitrate was highly correlated with ($R_p^2 \geq 0.95$) the total AMS

73   nitrate concentration and followed the 1 to 1 line for each method we used. Even though organic

74   nitrates also contributed to the total nitrate we measured, both the variation and the concentration

75   of the nitrate did not change significantly after subtracting the organic nitrates. Furthermore, as

76   shown in Fig. S2, AMS measured nitrate were comparable to those from MAGRA, with a

77   correlation slope of 0.9 and an R_p of 0.95. Given the uncertainties associated with each estimations,

78   we prefer to use the total HR-ToF-AMS nitrate concentration in our discussion.

79

80   **Figures and Tables:**

81

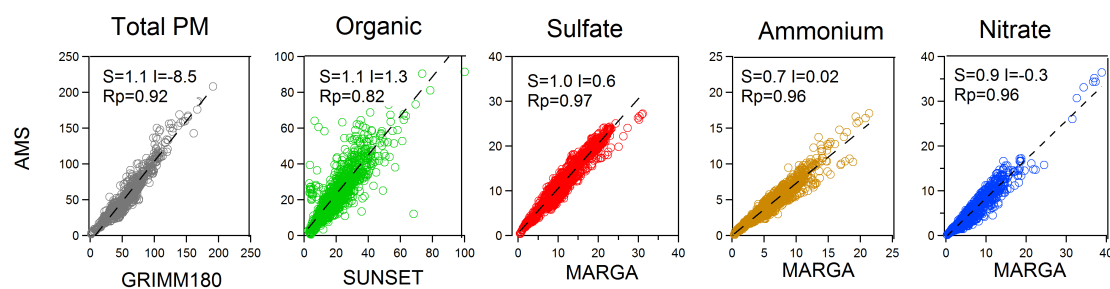82

83 *Figure S 1 Location of sampling site*
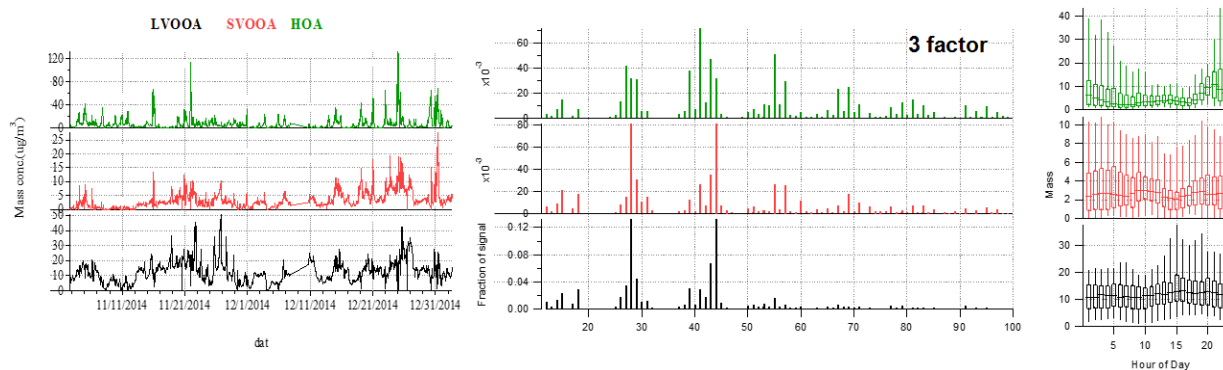
84

85

86

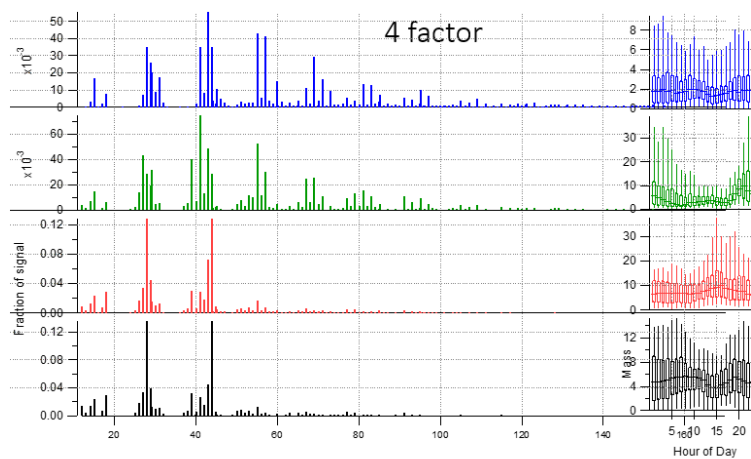87 *Figure S 2 AMS data comparison*
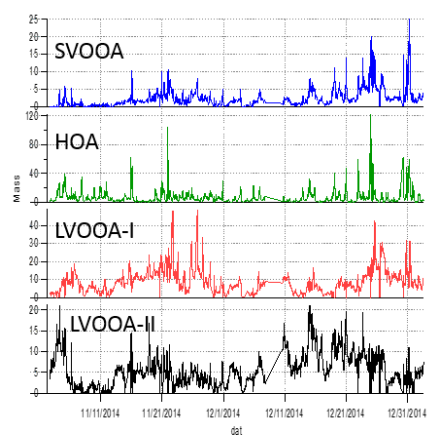

88

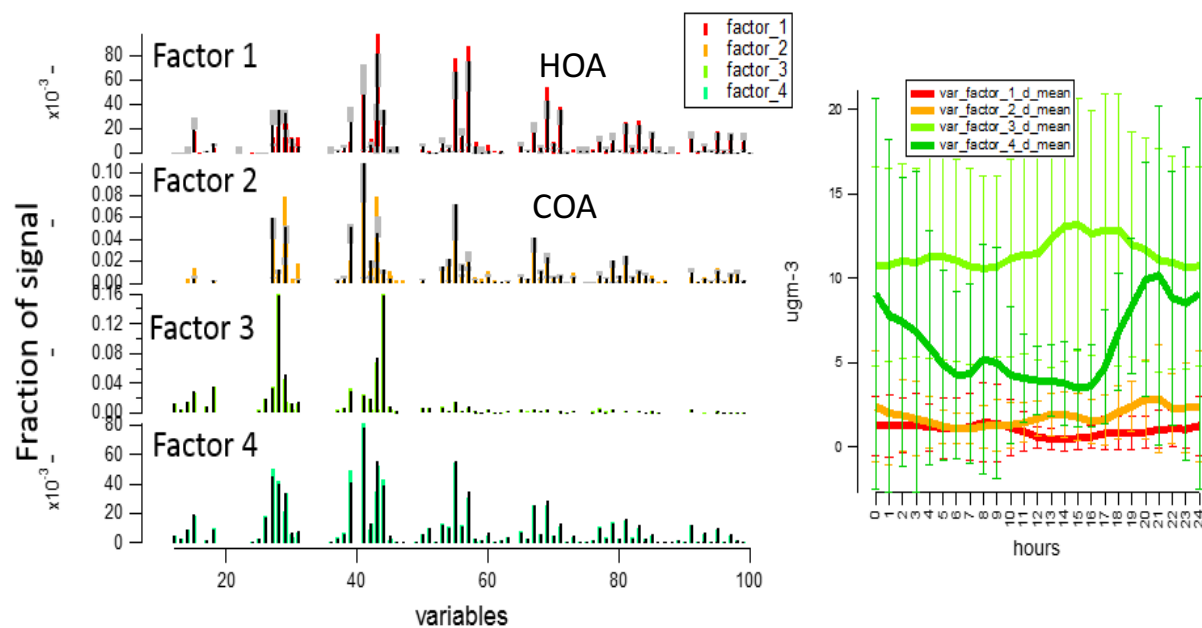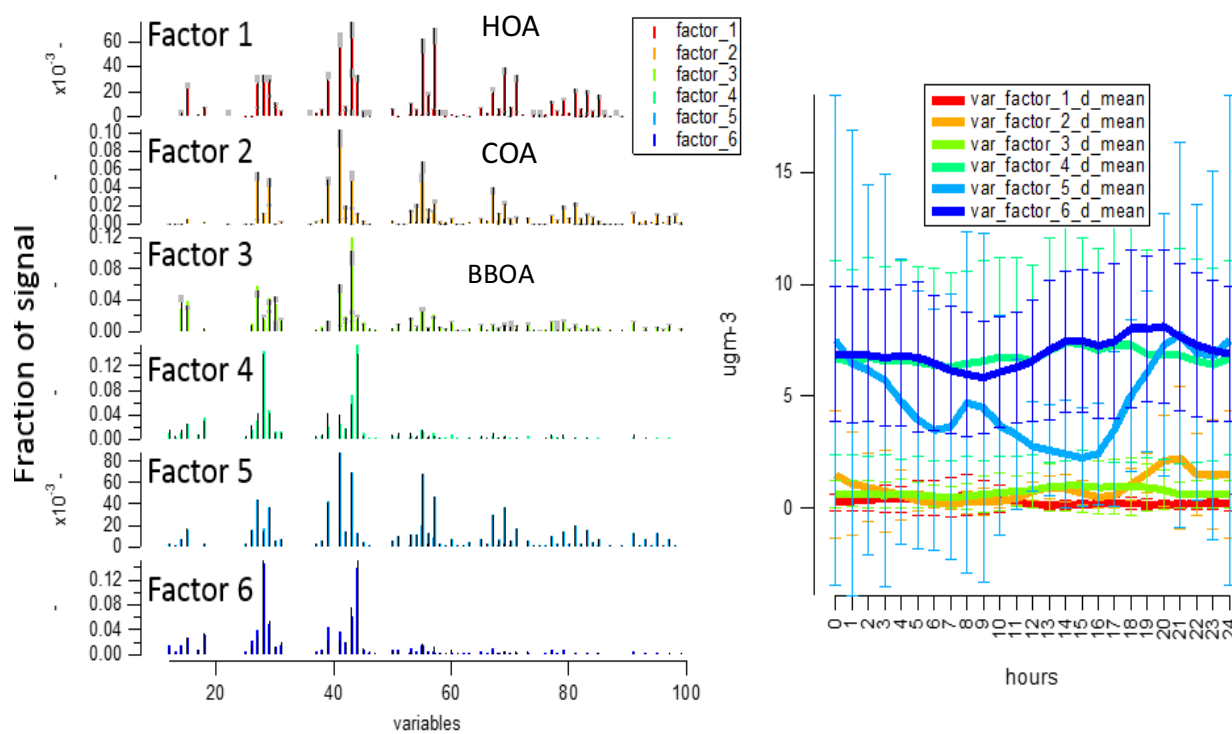89 *Figure S 3 Three factors PMF solution*

90
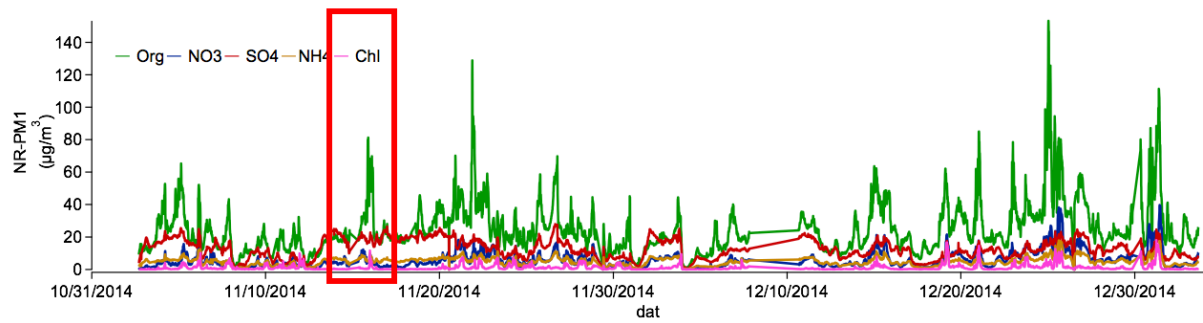
91   *Figure S 4 Four factors PMF solution*
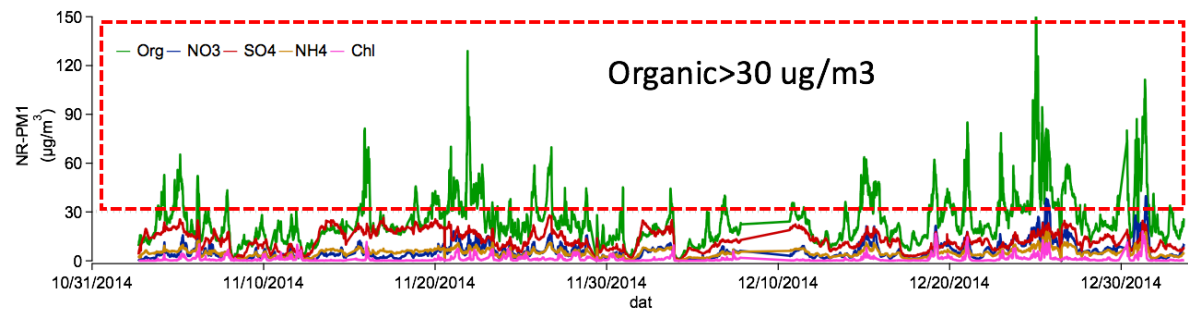
92

93

94 *Figure S 5 Factor profiles and diurnal variations in ME-2 trials. upper panel: four factor solution with constraining HOA and COA.*
95 *bottom panel: six factor solution with constraining HOA, COA and BBOA.*
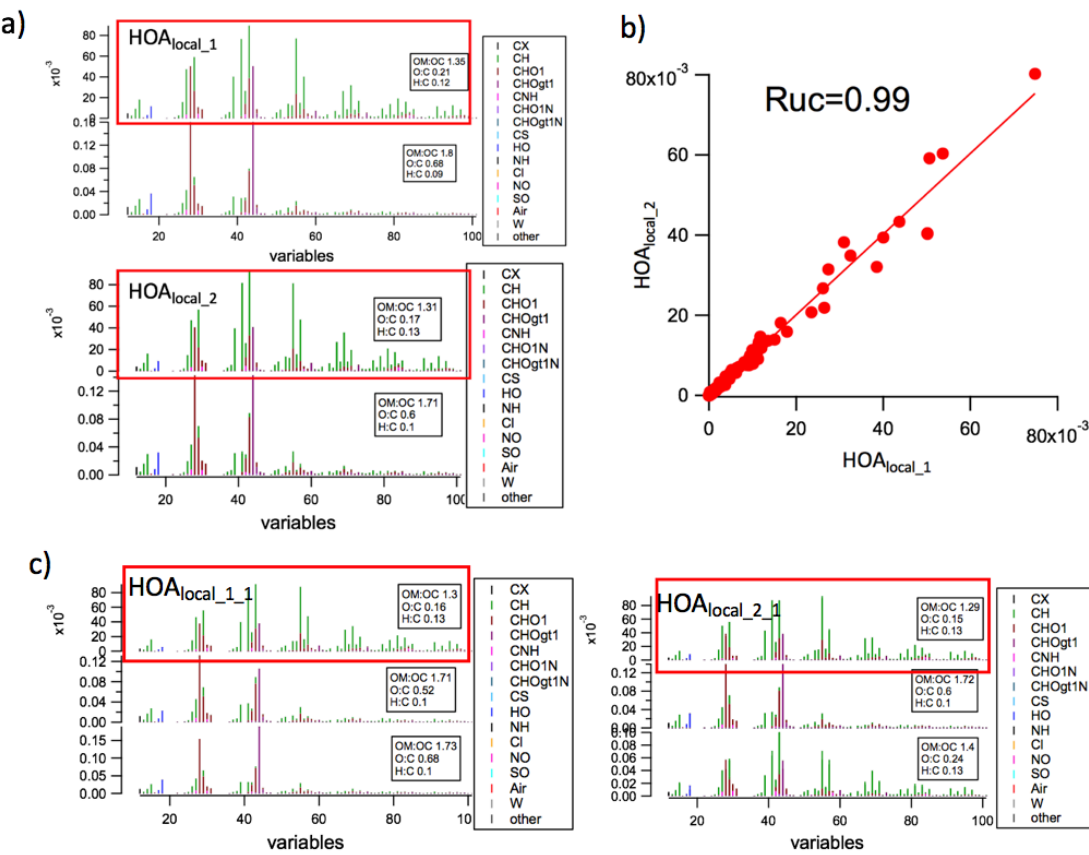
96

97

98 *Figure S 6 Organic peaks during the campaign*

101   *Figure S 7 Local HOA source profile comparison*
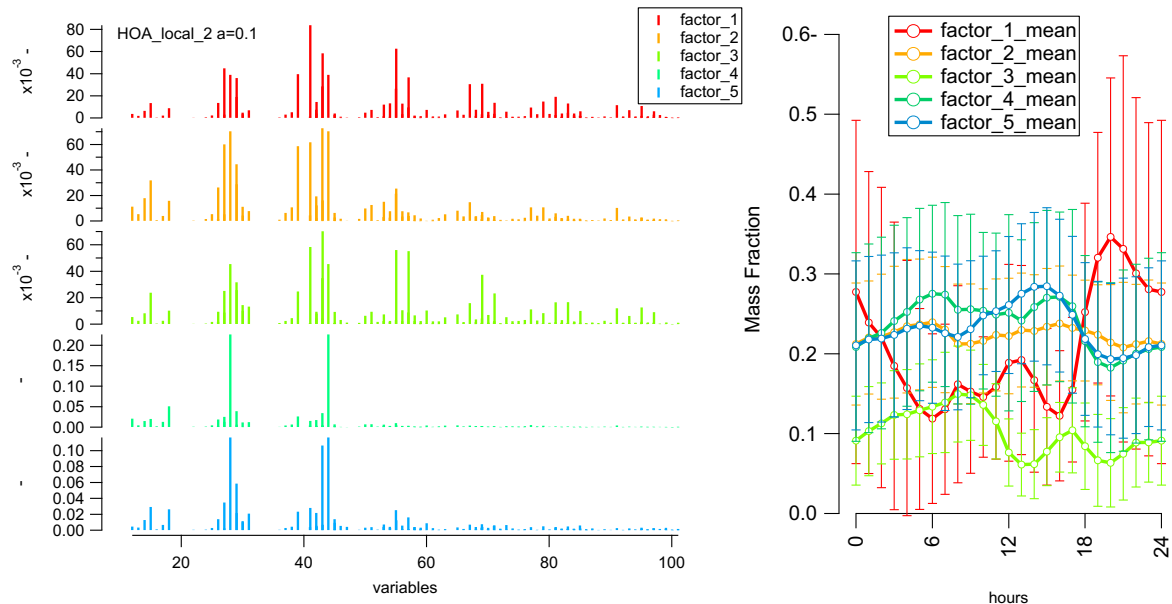
104   *Figure S 8 Five factor solution with HOA constrain*
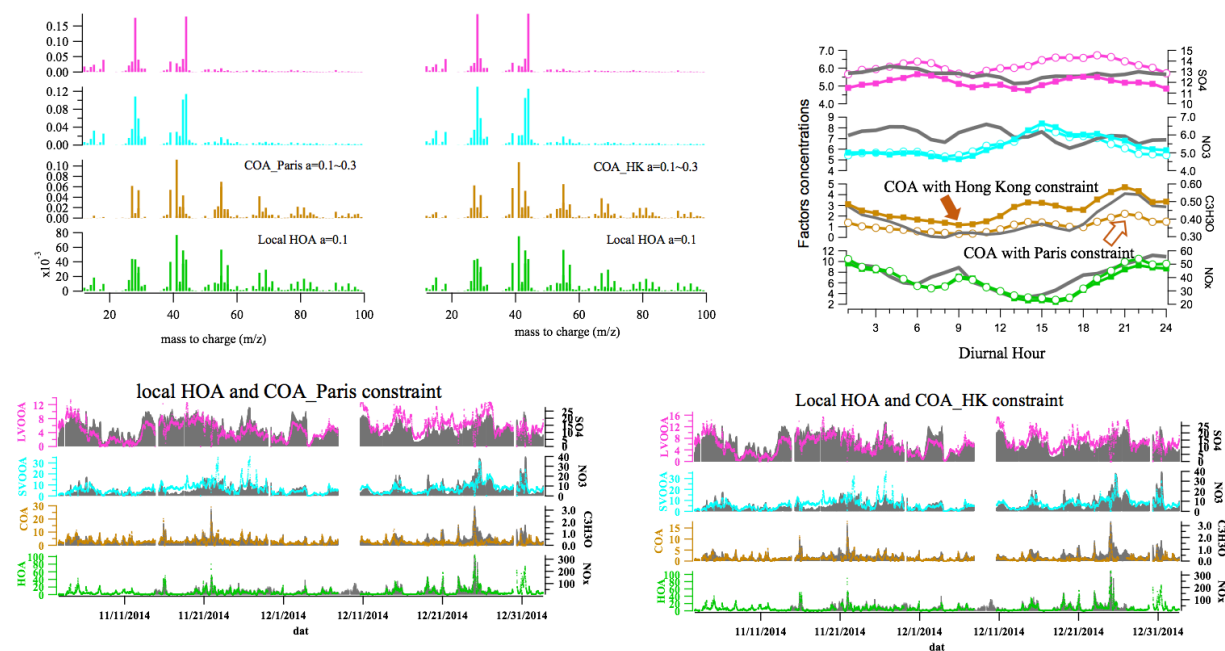
105
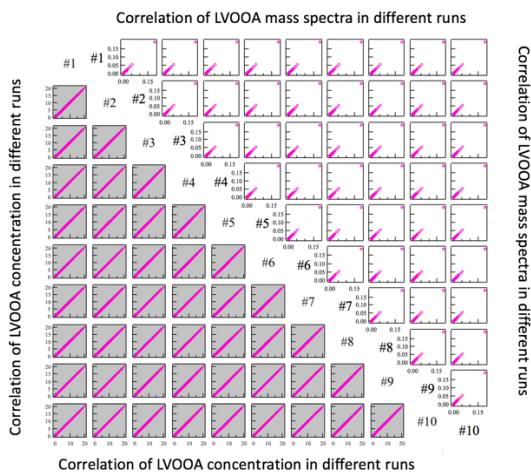106   *Figure S 9 ME-2 results comparison using the two COA source profile as constraint*
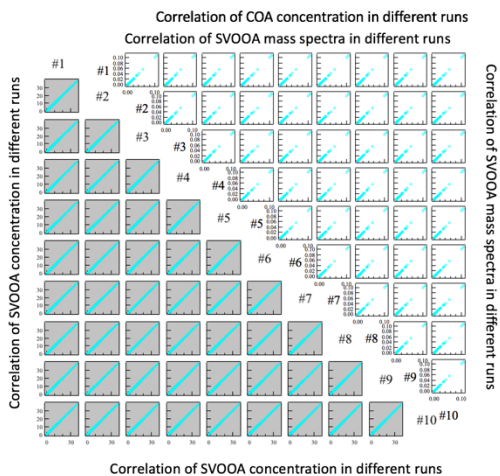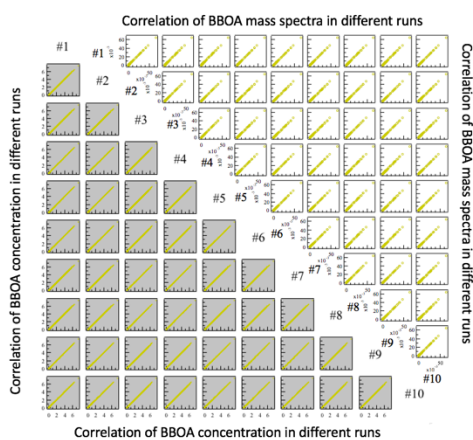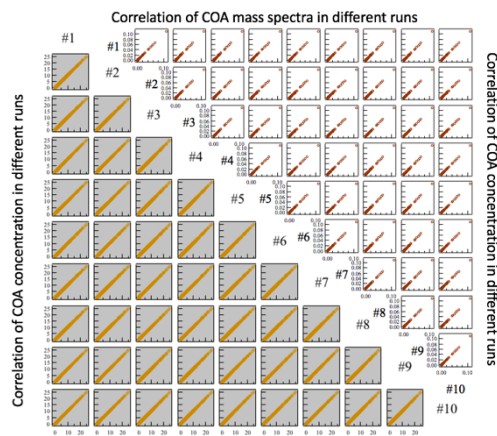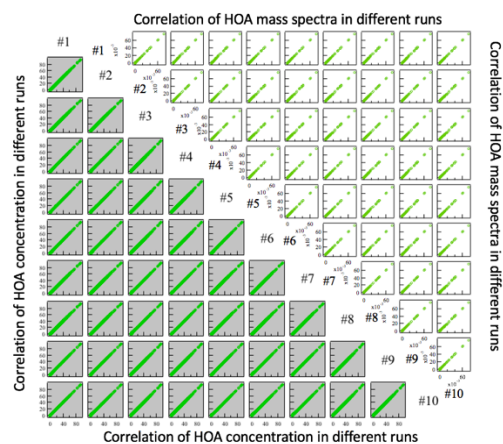
107

108

109
110

Figure S 10 Correlation of the time series and mass spectra for ten runs with optimal solution.
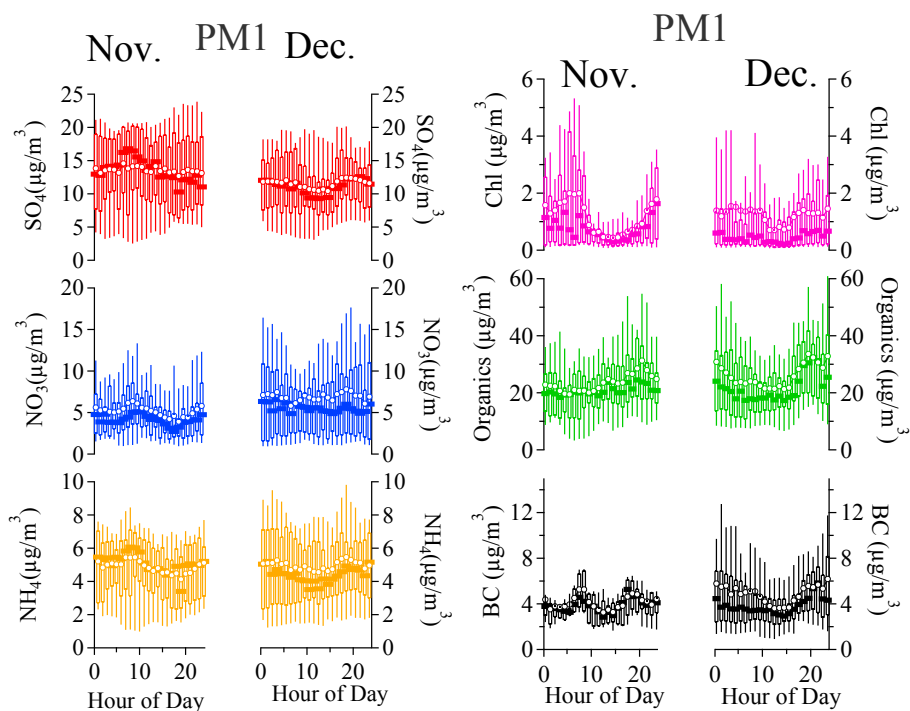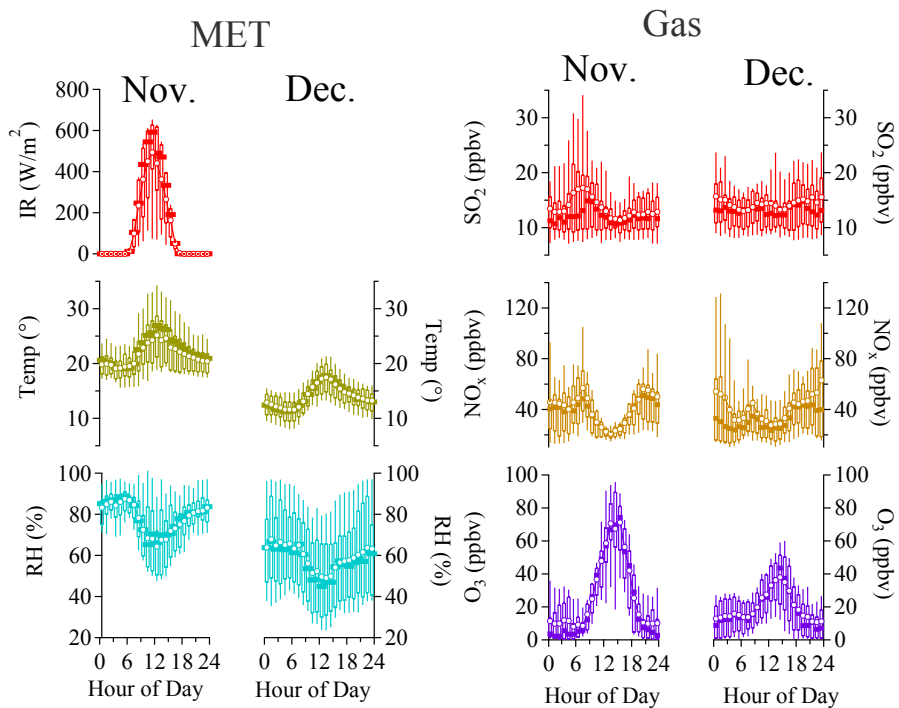
111

112

Figure S 11 *Diurnal patterns for temperature, RH, Irradiance, NOₓ, O₃, all NR-PM₁ species, and BC in Nov. and Dec. (25th and 75th percentile boxes,5th and 95th percentile whiskers, median as line in solid dot, and mean as cycle). There is no Irradiance data available in December*

113
114
115

116
117

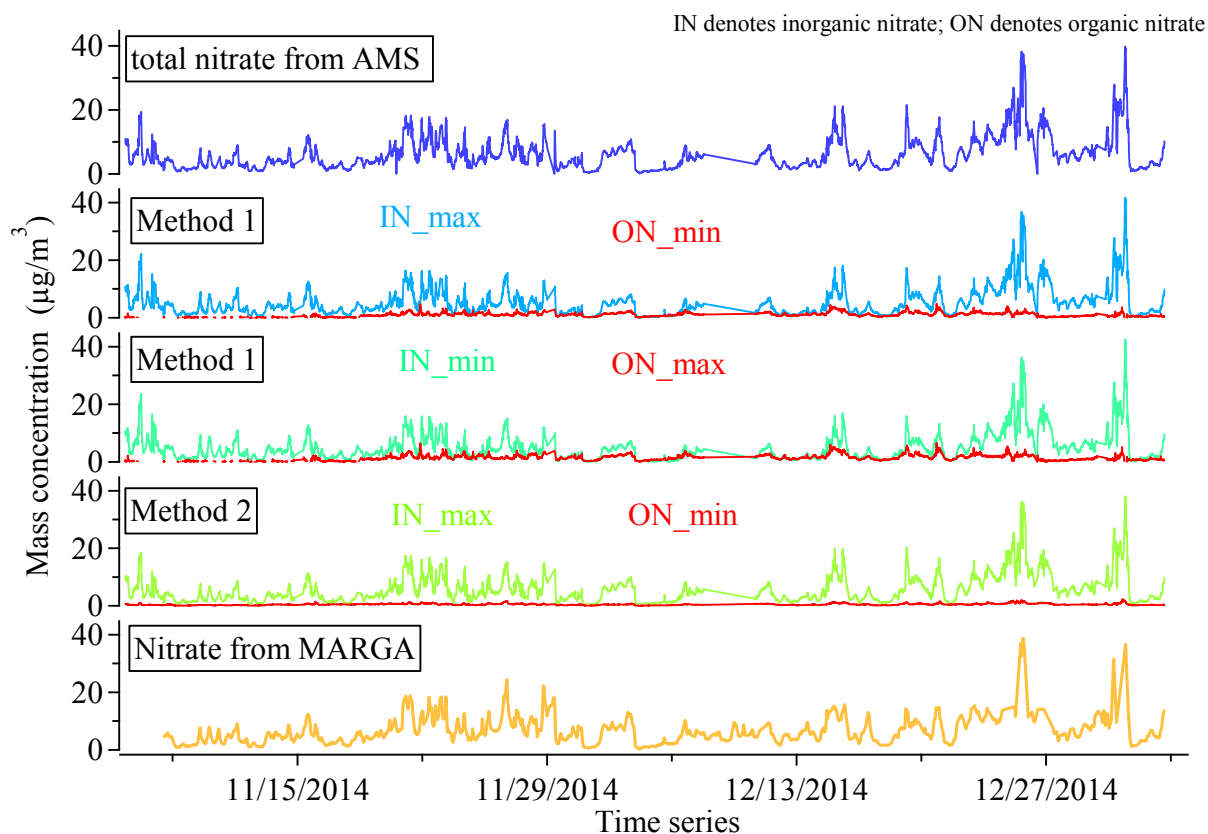IN denotes inorganic nitrate; ON denotes organic nitrate

118

Figure S 12 Time series of total nitrate form AMS and MAGRA and , inorganic nitrate and organic nitrate calculated from Method
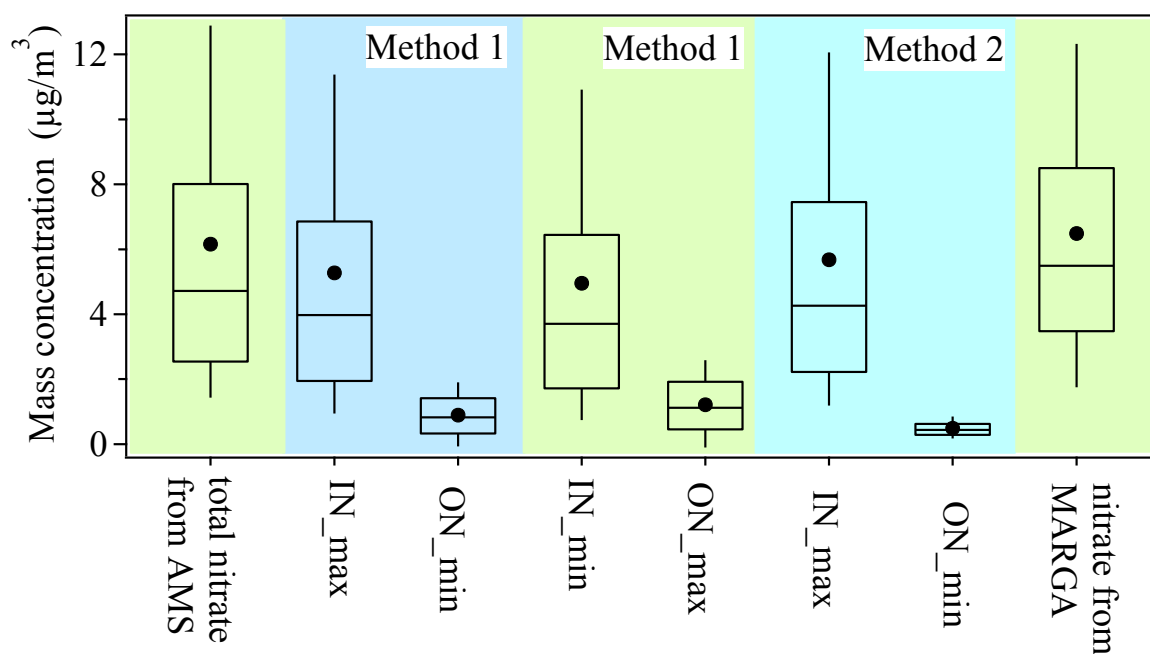*1 and Method 2. IN denotes inorganic nitrate and ON denotes organic nitrate.*

121

122

123 *Figure S13 Box and whisker plot of nitrate mass concentration from AMS and MAGRA, and inorganic nitrate and organic nitrate*
124 *calculated from Method 1 and Method 2 (25th and 75th percentile boxes, 10th and 90th percentile whiskers, median as line in solid*
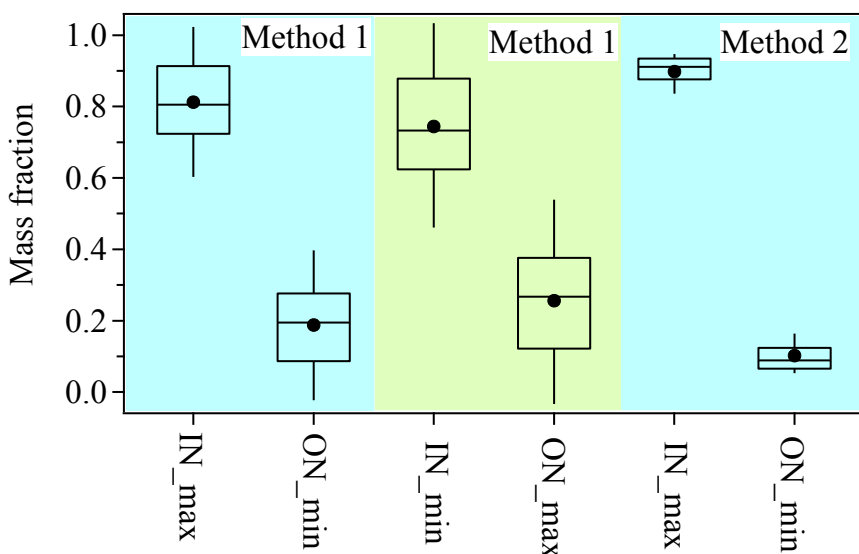125 *line, and mean as dot).*

126

127 *Figure S14 Box and whisker plot of inorganic nitrate and organic nitrate mass fraction calculated from Method 1 and Method 2*
128 *(25th and 75th percentile boxes, 10th and 90th percentile whiskers, median as line in solid line, and mean as dot).*

129

130

131   *Table S 1 Correlation of ME-2 resolved OA factors with tracers*

132

Correlation (R_p)	NO_x	C_3H_3O	$C_2H_4O_2$	NO_3	SO_4
HOA	0.83	0.84	0.81	0.58	0.18
COA	0.51	0.66	0.42	0.08	0.08
BBOA	0.18	0.47	0.71	0.52	0.33
LVOOA	-0.01	0.31	0.42	0.43	0.7
SVOOA	0.21	0.66	0.62	0.68	0.49

133

134

135

136

137

138

139 **Reference:**

140 Farmer, D. K., Matsunaga, a, Docherty, K. S., Surratt, J. D., Seinfeld, J. H., Ziemann, P. J. and

141 Jimenez, J. L.: Response of an aerosol mass spectrometer to organonitrates and organosulfates and

142 implications for atmospheric chemistry., Proc. Natl. Acad. Sci. U. S. A., 107(15), 6670–6675,

143 doi:10.1073/pnas.0912340107, 2010.

144 He, L.-Y., Huang, X.-F., Xue, L., Hu, M., Lin, Y., Zheng, J., Zhang, R. and Zhang, Y.-H.:

145 Submicron aerosol analysis and organic source apportionment in an urban atmosphere in Pearl

146 River Delta of China using high-resolution aerosol mass spectrometry, J. Geophys. Res., 116(D12),

147 D12304, doi:10.1029/2010JD014566, 2011.

148 Schurman, M. I., Lee, T., Desyaterik, Y., Schichtel, B. A., Kreidenweis, S. M. and Collett, J. L.:

149 Transport, biomass burning, and in-situ formation contribute to fine particle concentrations at a

150 remote site near Grand Teton National Park, Atmos. Environ., 112, 257–268,

151 doi:10.1016/j.atmosenv.2015.04.043, 2015.

152 Seinfeld, J. H. and Pandis, S. N.: ATMOSPHERIC From Air Pollution to Climate Change

153 SECOND EDITION., 2006.

154 Xu, L., Suresh, S., Guo, H., Weber, R. J. and Ng, N. L.: Aerosol characterization over the

155 southeastern United States using high-resolution aerosol mass spectrometry: spatial and seasonal

156 variation of aerosol composition and sources with a focus on organic nitrates, Atmos. Chem. Phys.,

157 15(13), 7307–7336, doi:10.5194/acp-15-7307-2015, 2015.

158